Photodissociation of CH_3OCl to $CH_3O + Cl$ at 248 nm

M. J. Krisch, L. R. McCunn, K. Takematsu, and L. J. Butler*

James Franck Institute and Department of Chemistry, The University of Chicago, Chicago, Illinois 60637

F. R. Blase

Haverford College, Department of Chemistry, Haverford, Pennsylvania 19041

J. Shu

Chemical Sciences Division, Lawrence Berkeley National Laboratory, Berkeley, California 94720

Received: October 23, 2003; In Final Form: December 29, 2003

This study examines the 248 nm photodissociation of methyl hypochlorite (CH_3OCl), a molecule that serves as an atmospheric chlorine reservoir. The data show that the primary photodissociation channel is cleavage of the O−Cl bond to produce Cl atoms and CH_3O radicals, a result consistent with the direct dissociation mechanism found by other computational and experimental studies of alkyl hypohalites. Photofragment translational spectroscopy with a crossed laser-molecular beam apparatus, coupled with tunable VUV photoionization detection, identified the momentum-matched products at $m/e = 35$ (Cl^+ from Cl atoms) and $m/e = 29$ (the CHO^+ daughter ion of CH_3O). Products were formed with a narrow range of recoil kinetic energies, peaking at 48 kcal/mol in the center-of-mass reference frame, with a full-width half-maximum of 4 ± 2 kcal/mol. This kinetic energy distribution shows that the CH_3O products are formed with a very narrow range of internal energies, and a simple model shows that to conserve angular momentum this internal energy, near 20 kcal/mol, is partitioned primarily to rotational energy. Thus CH_3OCl could serve as a photolytic precursor of CH_3O radicals with high and well-defined rotational and translational energies.

I. Introduction

Chlorinated compounds have long been understood to play a crucial role in atmospheric chemistry. One well-studied example of this is in the atmospheric cycles related to ozone formation and destruction. The roles of Cl and ClO have been investigated extensively; high concentrations of these species are prevalent in perturbed regions of the stratospheric ozone layer, such as those observed during the austral spring.[1−3] These radicals catalyze ozone loss, a process which is slowed by deactivation of Cl through various reactions with CH_4,[4] such as those shown in reactions 1 and 2.

$$CH_4 + Cl \rightarrow CH_3 + HCl \quad (1)$$

$$CH_4 + Cl + O_2 \rightarrow CH_3O_2 + HCl \quad (2)$$

More recently, it has become evident that alkyl hypochlorites can also influence stratospheric chemistry through their involvement in methane oxidation chemistry and their role as reservoirs of Cl. Crutzen et al. first demonstrated computationally that the gas-phase reaction between CH_3O_2 and ClO might play a role in ozone chemistry.[4] This suggestion was confirmed in kinetics experiments by Kenner et al.[5] and Helleis et al.,[6,7] which found that the reaction proceeded through two channels:

$$CH_3O_2 + ClO \rightarrow CH_3O + ClOO \quad (3a)$$

$$CH_3O_2 + ClO \rightarrow CH_3OCl + O_2 \quad (3b)$$

Though early experiments[8,9] were unable to detect the weakly absorbing, unstable CH_3OCl products from reaction 3b, later work using a discharge flow/mass spectrometer apparatus showed that this channel accounts for ∼23% of the reaction at typical stratospheric temperatures of ∼200 K.[7] Helleis et al. obtained a channel-specific rate constant of $(4.1 \pm 1) \times 10^{-13}$ cm^3 $molecule^{-1}$ s^{-1}.[7] These measurements indicate that channel 3b may have a significant impact on stratospheric chlorine cycles.

Any attempt to elucidate the role of CH_3OCl in stratospheric chemistry leads to the question of what loss mechanisms exist for this molecule in the atmosphere. The rate of reaction between CH_3OCl and Cl was measured by Carl et al.[10] and found to be relatively high, with a rate constant of $(6.1 \pm 0.6) \times 10^{-11}$ cm^3 $molecule^{-1}$ s^{-1} at 295 K. This rate constant was determined at a higher temperature than those typical of the stratosphere but the authors propose that in analogy with the $Cl + Cl_2O$ reaction, the rate constant for the $CH_3OCl + Cl$ reaction is likely to have a weak temperature dependence. Their findings suggest that reaction with Cl may serve as an important CH_3OCl removal process in the stratosphere. The reaction between CH_3OCl and OH appears to be less important; a study by Crowley et al.[11] found it to have a relatively low rate constant, $k(250-341\ K) = (2.4 \pm 0.8) \times 10^{-12} \exp(-(360 \pm 100)/T)$ cm^3 $molecule^{-1}$ s^{-1}, which can be extrapolated to a value of 4×10^{-13} cm^3 $molecule^{-1}$ s^{-1} at 200 K.

In addition to collisional energy loss, photochemical loss processes are expected to play an important role in destroying CH_3OCl. This can be evaluated through examination of the ultraviolet (UV) absorption spectrum of CH_3OCl. Crowley et al.[12] characterized the UV absorption spectrum of gas-phase CH_3OCl from 200 to 460 nm. A study by Jungkamp et al.[13]

10.1021/jp0372082 CCC: $27.50
Published on Web 00/00/0000 PAGE EST: 6.6

measured the gas-phase absorption cross-sections of a series of hypochlorites, including methyl hypochlorite, in the wavelength range 230−400 nm. The two studies were in qualitative agreement, with a slight discrepancy regarding the cross-section at wavelengths shorter than ∼250 nm. The absorption cross section of CH_3OCl at 248 nm was found to be 1.17×10^{-19} cm^2 $molecule^{-1}$ by Jungkamp et al.[13] and 1.28×10^{-19} cm^2 $molecule^{-1}$ by Crowley et al.[12] The absorption spectrum exhibited two peaks in the UV range, one centered at 235 nm and a weaker one peaking at 310 nm. Crowley et al.[12] calculated a photolysis rate constant of 6.8×10^{-5} s^{-1} at a pressure of 100 mbar and a zenith angle of 80°, resulting in a stratospheric lifetime for CH_3OCl of 4.1 h. The addition of perturbed ozone conditions (i.e., gas concentrations typical of the development of an ozone hole) into this simulation was not found to alter the photolysis rate constants greatly, as the 310 nm peak was responsible for the bulk of atmospheric photodissociation. The stronger absorption at shorter wavelengths was always at least partially screened by ozone. The calculated photolysis rates are comparable to reaction rates of $Cl + CH_3OCl$ at Cl concentrations of $\sim 1 \times 10^6$ cm^{-3}.[10] In comparison, the $OH + CH_3OCl$ reaction appears to be a negligible loss process in the stratosphere, because at OH concentrations of $\sim 1 \times 10^6$ cm^{-3} the removal rate of CH_3OCl would be 4×10^{-7} s^{-1}, corresponding to a lifetime of about 29 days.[11]

Further information regarding the UV absorption of CH_3OCl comes from a computational study by Li and Francisco,[14] which characterized the first eight electronic states of CH_3OCl. From these computations, they were able to assign two of the absorption peaks in the CH_3OCl UV spectrum. They assigned the 310 nm feature to a $\tilde{X}\ ^1A' \rightarrow 1^1A''$ transition, which is predominantly characterized by excitation of an electron from an out-of-plane nonbonding p orbital on the Cl to an in-plane O−Cl antibonding orbital ($4a'' \rightarrow 14a'$). The 235 nm peak was attributed to a $\tilde{X}\ ^1A' \rightarrow 2^1A'$ transition corresponding to excitation of an electron from an in-plane nonbonding p orbital on Cl and to an in-plane O−Cl antibonding orbital ($13a' \rightarrow 14a'$).

Structural and energetic information about CH_3OCl is available from several computational studies.[15−18] Several decomposition pathways are found to be energetically possible following excitation at 248 nm, as shown below, where ΔE values are energies relative to ground-state CH_3OCl (with no zero point correction) as calculated by He et al.[17] at the G2MP2 level. Many of these reactions are also considered by Jung et al.[18]

$$CH_3OCl \rightarrow CH_3O + Cl \qquad \Delta E = 50.45 \text{ kcal/mol} \quad (4a)$$

$$CH_3OCl \rightarrow HCl + CH_2O \qquad \Delta E = -33.93 \text{ kcal/mol} \quad (4b)$$

$$CH_3OCl \rightarrow CH_2ClOH \qquad \Delta E = -43.22 \text{ kcal/mol} \quad (4c)$$

$$CH_3OCl \rightarrow H_2 + CHOCl \qquad \Delta E = 39.66 \text{ kcal/mol} \quad (4d)$$

$$CH_3OCl \rightarrow CH_3 + OCl \qquad \Delta E = 78.11 \text{ kcal/mol} \quad (4e)$$

$$CH_3OCl \rightarrow CH_2 + HOCl \qquad \Delta E = 89.62 \text{ kcal/mol} \quad (4f)$$

$$CH_3OCl \rightarrow CH_2OCl + H \qquad \Delta E = 100.82 \text{ kcal/mol} \quad (4g)$$

Despite the numerous energetically allowed pathways, it is likely that pathway 4a, O−Cl bond fission, will follow from UV excitation, as calculations[14] find that the first several singlet and triplet excited states of CH_3OCl, including the bright $2^1A'$ state accessed at 248 nm, are highly repulsive along the O−Cl bond coordinate. Support for this conjecture is given by two experimental studies, one that examined UV photolysis of CH_3OCl in a time-of-flight mass spectrometer[19] and the other that performed photofragment translational spectroscopy on an analogous compound, *tert*-butyl hypochlorite.[20] Both studies observed only direct O−Cl bond fission. It is also worth noting that the qualitative shape of the UV absorption spectrum is quite similar for several alkyl hypochlorites studied,[13,20] which suggests that they access analogous repulsive excited electronic states and will exhibit similar behavior upon photolysis.

The previous photodissociation study of CH_3OCl by Schindler et al.[19] was able to gain an estimate of the translational energy of the Cl fragments and to clearly characterize the spin−orbit population ratio of excited-state chlorine, $Cl(^2P_{1/2})$, to ground-state chlorine, $Cl(^2P_{3/2})$, as 1.45 ± 0.05 after excitation at ∼236 nm. They were unable to detect the expected CH_3O cofragments, however; CH_3O did not give a detectable REMPI signal. The apparatus used in the study combined UV/vis absorption measurements in a drift tube under pressures of 5−40 mbar with mass spectrometric determination of the photoproducts. Gas from the UV/vis section of the experiment was introduced into a commercial Bruker TOF1 mass spectrometer via a pulsed shutter (the final pressure in the mass spectrometer was not specified). An estimate of the mean recoil velocity of the Cl atoms was obtained from the difference in turnaround times of the ionized photofragments when an electric field was applied (the TOF profiles of photodissociated Cl atoms were similar in shape to those in thermal equilibrium with the carrier gas). The current study extends the investigation of Schindler et al. by examining CH_3OCl photolysis at 248 nm after cooling in a supersonic jet, in an apparatus where momentum-matched photolysis products can be observed under collisionless conditions and the shape of the recoil translational energy distribution, $P(E_T)$, can be determined. From this, we deduce the internal energy distribution of the CH_3O radical cofragments and gain insight into their rotational and vibrational energy content.

II. Experimental Section

A. Synthesis of Methyl Hypochlorite. Methyl hypochlorite (CH_3OCl) is light sensitive, has a low boiling point (12 °C), and is highly unstable at high concentrations. As a precaution, procedures were performed at low light levels and CH_3OCl was stored as a dilute solution in dichloromethane (CH_2Cl_2) at $T <$ 0 °C. All glassware and reagents were chilled in an ice bath to $T <$ 10 °C before use (with the exception of acetic acid, which freezes at 16.6 °C, and the filtration apparatus which included a filter flask and a Büchner funnel). Anhydrous dichloromethane (Acros, 99.9%), methanol (Fisher Scientific), glacial acetic acid (Fisher Scientific), and NaOCl (Ultra Clorox Regular) were purchased from commercial sources and used without further purification.

Methyl hypochlorite (CH_3OCl) was synthesized according to modified procedures from previously published reports.[21,22] Anhydrous dichloromethane (200 mL) was added to a cold 500 mL Erlenmeyer flask equipped with a stir bar. The flask was cooled in an ice bath and cold methanol (8 mL) and glacial acetic acid (12 mL) were added in one portion to the chilled CH_2Cl_2. The resulting solution was mixed well and stirred at 0 °C for 5 min, after which time it was carefully poured into a separate, chilled, 1 L round-bottom flask containing ice-cold commercial bleach (220 mL, 6% NaOCl). The biphasic mixture was vigorously stirred for 3 min at 0 °C and then transferred to a chilled separatory funnel. Extractions were performed quickly to avoid decomposition of the methyl hypochlorite. The aqueous layer was immediately discarded. The organic layer was washed

with 10% aq $NaHCO_3$ (3 × 100 mL) to neutralize any remaining acetic acid, washed with H_2O (1 × 50 mL), dried over anhydrous Na_2SO_4 (5 g) for 5 min, and then filtered through glass-fiber filter paper (Schleicher & Schuell, Grade 30) to ensure quick but highly efficient filtration. The solid sodium sulfate was rinsed thoroughly with anhydrous cold dichloromethane (~50 mL), and the resulting yellow organic filtrate was immediately transferred to a prechilled, dry, brown-glass bottle and stored in a freezer at $T < 0$ °C.

The CH_3OCl solution prepared above was determined to be 0.6 M concentration by iodometric titration with aqueous $Na_2S_2O_3$. A mass spectrum of the solution was taken, on the apparatus described below, with 15.1 eV VUV photoionization to confirm that signal was observed at $m/e = 66$, corresponding to the parent. Water signal was observed but may have been introduced either in the synthesis or during preparation of the molecular beam. CH_3OCl signal was observed, through consecutive mass spectra, to decay on the order of days.

B. Photofragment Translational Spectroscopy. The recoil velocity distributions of photofragments from CH_3OCl photodissociation at 248 nm were measured in a crossed laser-molecular beam scattering apparatus. Experiments were performed at Endstation 1 of the Chemical Dynamics Beamline of the Advanced Light Source (ALS) at the Lawrence Berkeley National Laboratory.[23,24] Photodissociation occurred at an "interaction region" in which the laser beam intersected a molecular beam. The propagation axis of the laser beam was perpendicular to the plane containing the molecular beam and the line from the interaction region to the detector. The source region containing the molecular beam nozzle was continuously rotatable to allow for data collection at different values of the source angle, defined as the angle between the molecular beam propagation axis and the line from the interaction region to the detector. Photodissociation products scattered into many angles; the apparatus sampled only the small portion of products with lab velocities pointed along the interaction region-to-detector line within the 1.3° acceptance angle of the detector. Photolysis products traveled 15.1 cm to a detector that used tunable vacuum-ultraviolet (VUV) photoionization. The ions passed through a 2.1 MHz quadrupole mass spectrometer; the resolution varied slightly with mass and was set to avoid problems of mass leakage at all masses of interest (the full-width half-maximum, fwhm, at $m/e = 29$ was 0.36 amu). The mass-selected ions were detected by a Daly detector, and the resultant voltage pulses were counted by a multichannel scaler. This gave the number of ions at each mass to charge (m/e) ratio produced from the neutral photofragments arriving at the detector, as a function of time after the dissociating light pulse. An ion flight time constant of 7.02 μs/amu$^{1/2}$ was used to correct for the portion of the photofragment's travel during which it was an ion; the sum of neutral and ion flight times are given in the figures herein. The time-of-flight spectra of the photofragments were forward convolution fit to determine the distribution of energies partitioned to the neutral photofragment recoil translational energy.

The synchrotron radiation was generated with a U10 undulator and tuned through changes in the undulator gap. In addition to radiation at the wavelength of interest, higher harmonic light was generated. An argon gas filter helped to block out these higher harmonics, but at many values of the m/e ratio this was not sufficient, so background subtraction was used. Background was acquired by running the laser at half the repetition rate of the pulsed valve and collecting signal when the molecular beam was on and the laser was off. The photoionization energies quoted here are determined from the undulator gap and related to the energy by a recent calibration done with a 3 m McPherson monochromator with a 600 groove/mm grating.[25] This is not equivalent to the values given by the beamline "calculator", which were reported in many previous publications from this apparatus and which deviate significantly from the true value in some cases. For example, when the beamline calculator is set to give 15.0 eV, the actual center energy is about 0.3 eV lower than that. For the spectra taken here, beam defining apertures of 10 mm × 10 mm were used to spatially select a portion of the ALS beam, giving a total spectral bandwidth of about 5% fwhm. Most of the width beyond 2.3% fwhm, however, arose from a long tail extending out to the red.[25]

The KrF transition of an unpolarized excimer laser produced the 248.5 nm light used for photolysis. Data were collected at laser energies of 20 and 80 mJ pulse^{-1} focused onto a 5.8 mm^2 spot. Power studies from 14 to 90 mJ at $m/e = 35$ (Cl^+) found that signal intensity varied linearly with laser power, confirming that the observed $m/e = 35$ signal resulted from single photon dissociation of CH_3OCl.

Signal from the photofragmentation of methyl hypochlorite was observed at $m/e = 35$ (Cl^+) and $m/e = 29$ (CHO^+). No evidence was found for signal at $m/e = 31$ (CH_3O^+) or $m/e = 30$ (CH_2O^+) (see Results and Analysis for further discussion).

A 0.6 M solution of CH_3OCl in CH_2Cl_2 was synthesized as described above and kept at a temperature of −23 °C. The vapor at equilibrium with the solution was seeded in He to a total backing pressure of 400 Torr and expanded through an unheated pulsed nozzle of 1 mm orifice diameter (180 μs pulse length). The CH_2Cl_2 absorption at 248 nm is negligible ($\sigma < 2 \times 10^{-22}$ cm^2).[26] The speed distribution of molecules in the molecular beam was measured with a chopper wheel for each spectrum; for the Cl^+ data it had a peak at 1033 m/s in the number density distribution $N(v)$, with a fwhm of 15.3%. The CHO^+ data were taken with a faster beam, with a peak in $N(v)$ at 1057 m/s and a fwhm of 18.0%.

Calculations to find the bond dissociation energy of CH_3OCl were performed using GAUSSIAN 98[27] at the G3//B3LYP level of theory, as described by Baboul et al.[28] The average absolute deviation of G3//B3LYP calculated heats of formation against the G2/97 test set (148 enthalpy values) was 0.93 kcal/mol.[28]

III. Results and Analysis

Photofragment translational energy spectra showed evidence for only one bond fission channel arising from the photolysis of methyl hypochlorite (CH_3OCl) at 248.5 nm. All data could be fit under the assumption that only cleavage of the Cl−O bond occurred to produce Cl and the methoxy radical (CH_3O). This is consistent with the highly repulsive nature of the near UV excited states of CH_3OCl along the Cl−O bond coordinate.

Signal from the Cl atom photoproduct in O−Cl fission was observed at $m/e = 35$ (Cl^+) at source angles of 15° and 35° and a photoionization energy of 14.7 eV, with the 35° data shown in Figure 1. The $P(E_T)$ derived from forward convolution fitting of these spectra peaks sharply near 48 kcal/mol with a full width half-maximum of approximately 4 ± 2 kcal/mol (Figure 2). The shape of this distribution was constrained to a Gaussian, for ease of varying the peak position and width. The impulsive recoil of the Cl atom from the nascent CH_3O thus imparts considerable energy to relative translational energy and, as described in the Discussion, must also impart considerable energy to the rotation of CH_3O. The ionization energy of CH_3O, estimated from experimental values for the ionization energy

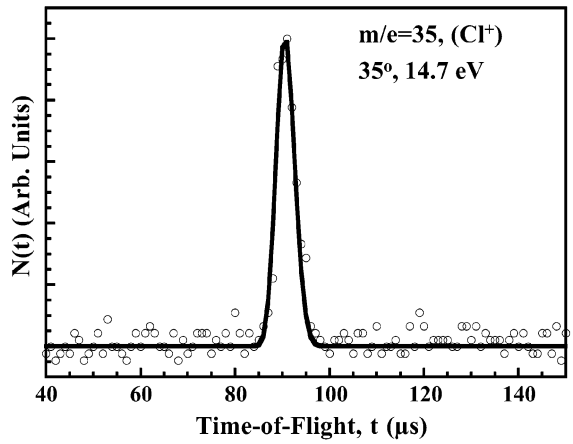

Figure 1. TOF spectra at $m/e = 35$ (Cl^+) at a source angle of 35° taken with photoionization energy of 15 eV, signal averaged for 434 750 laser shots. The forward convolution fit to these data, shown with a solid line, was obtained from the $P(E_T)$ shown in Figure 2. Experimental data points are given by open circles.

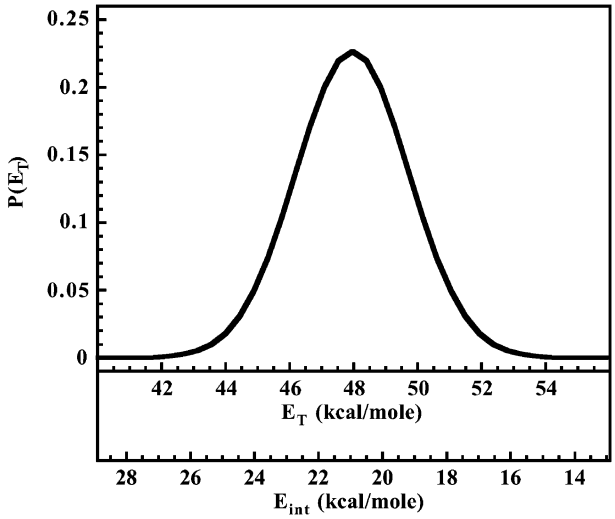

Figure 2. $P(E_T)$ for Cl−O bond fission, derived from the forward convolution fit of the $m/e = 35$ (Cl^+) spectra in Figure 1, is given by the solid line. Alternate fits of the spectra show that the peak of the $P(E_T)$ is determined to within ±1 kcal/mol and the full width at half-maximum is determined to be 4 ± 2 kcal/mol. The lower *x*-axis, calculated by eq 5, corresponds to the internal energy distribution of any CH_3O radicals with a $Cl(^2P_{3/2})$ cofragment.

of CD_3O, is reported as 10.7 eV.[29,30] CH_3O predominantly forms CHO^+ with large quantum yield.[31] We detected the momentum-matched partner of Cl, CH_3O, at $m/e = 29$ (CHO^+) at a source angle of 35° and a photoionization energy of 12.8 eV (Figure 3). The fact that these data were well fit using the $P(E_T)$ derived from the Cl^+ signal shows that the recoil velocities of all of the photofragments detected at $m/e = 29$ (CHO^+) correspond to daughter ions of CH_3O fragments, as the Cl and CH_3O must be momentum-matched, $m_{CH_3O}\vec{v}_{CH_3O} = -m_{Cl}\vec{v}_{Cl}$, in the center-of-mass reference frame. Little signal was detected for $m/e = 31$ (CH_3O^+) at a source angle of 15° after data were collected for 45 500 laser shots at photoionization energies of 11.4 and 12.8 eV. Assuming Poisson statistics, the total, background-subtracted signal at these photoionization energies was found to be −2 ± 3 counts and 11 ± 5 counts, respectively. We also looked for signal at $m/e = 30$ (CH_2O^+), because the AE of CH_2O^+ from CH_3O does not appear to be known. After data were collected for 50 000 laser shots at 12.8 eV and a source angle of 35°,

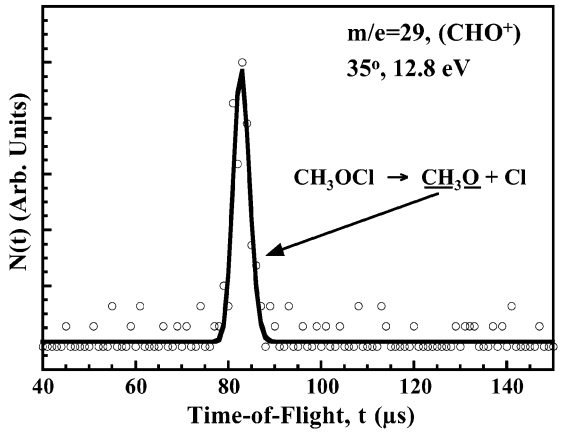

Figure 3. TOF spectra at $m/e = 29$ (CHO^+) at a source angle of 35° taken with photoionization energy of 13 eV with signal averaging 35 000 laser shots. The signal was momentum matched to signal from $m/e = 35$ (Cl^+) shown in Figure 1. The forward convolution fit to these data is shown with a solid line, whereas the experimental data points are given by open circles.

there was no evidence of any $m/e = 30$ (CH_2O^+) products. The total, background subtracted signal was found to be 8 ± 38 counts.

Although HCl elimination from CH_3OCl, with a barrier ≈53 kcal/mol,[17,18] might follow from vibrational excitation of CH_3OCl, we have no reason to expect that it would compete with direct dissociation along the C−O bond coordinate. Indeed, the study by Schindler et al.[19] set an upper limit of $\sigma^{HCl}_{248nm} < 0.01$ on the possible branching to HCl elimination. Although if a CH_2O cofragment was present from HCl elimination it might contribute to the signal at the daughter ion CHO^+ ($m/e = 29$), because the appearance energy of CHO^+ from CH_2O is 11.97 eV,[32] no daughter ion signal at $m/e = 29$ nor parent ion signal at $m/e = 30$ (CH_2O^+) from CH_2O was detected. All the signal in the CHO^+ TOF was fit by the O−Cl fission $P(E_T)$, and thus we conclude that there is no significant HCl elimination. We did not look for signal at $m/e = 36$ (HCl).

The internal energy of the nascent CH_3O photofragment formed upon O−Cl fission can be determined from the measured recoil energy distribution, $P(E_T)$ and conservation of energy:

$$E_{parent} + E_{h\nu} = D_{0(O-Cl)} + E_{int} + E_T \qquad (5)$$

Due to rotational cooling in the molecular beam, E_{parent} was taken to be equivalent to $\langle E_{vib}\rangle$ of the parent at the nozzle temperature, calculated to be 0.7 kcal/mol using vibrational frequencies from the literature[13,15] and a nozzle temperature of 298 K. $E_{h\nu}$ is the energy of the 248.5 nm excitation photon (115.1 kcal/mol). $D_{0(O-Cl)}$, the zero point-corrected bond dissociation energy, is found to be 47.0 kcal/mol from $\Delta H_f°_{0K}$ values calculated at the G3//B3LYP level of theory. There have been several computational determinations of ΔH_f values for CH_3OCl that are summarized in a study by Jung et al.[18] Our calculated value of $\Delta H_f°_{298K} = -14.47 \pm 1.5$ kcal/mol agrees to within the uncertainty of the two highest level estimates[16,18] (we recalculated it to determine D_0 entirely from $\Delta H_f°_{0K}$ values calculated at a single level of theory). From the $P(E_T)$ (Figure 2), it can be seen that between 42 and 54 kcal/mol was partitioned to recoil kinetic energy, E_T. Thus, the corresponding internal energy distribution, determined from eq 5, of the CH_3O fragment found in coincidence with the ground spin−orbit state Cl atom ranges from 15 to 27 kcal/mol, as shown in the double *x*-axis in Figure 2.

IV. Discussion

The photodissociation of CH_3OCl at 248 nm results in cleavage of the O−Cl bond. This study was the first to examine the width of the energy distribution for the photodissociation products. The resulting radicals were found to be nearly monoenergetic, with a fwhm of only 4 ± 2 kcal/mol in the recoil kinetic energy distribution. The partitioning of a large fraction of the available energy to recoil kinetic energy is consistent with a direct dissociation on an excited-state repulsive in the O−Cl bond. The spread in internal energies can be accounted for by internal excitation of either the CH_3O or the Cl fragments. The only energetically accessible way in which to internally excite the Cl atoms is to promote them to their first spin−orbit excited electronic state, $Cl(^2P_{1/2})$, which is separated from the ground state, $Cl(^2P_{3/2})$ by 2.5 kcal/mol. Previous work by Schindler et al.[19] found the $Cl(^2P_{1/2})/Cl(^2P_{3/2})$ ratio following photolysis at 235 and 238 nm to be 1.45 ± 0.05, so a substantial fraction of the Cl atoms are expected to be electronically excited. The zero point level of the first electronic excited state of the methoxy radical, $\tilde{A}\ ^2A_1$, lies 90.3897 ± 0.0001 kcal/mol[33,34] above the zero point level of the $\tilde{X}\ ^2E$ ground state, so electronic excitation of the methoxy radical is energetically inaccessible. Thus, the rest of the internal energy should be partitioned to internal rotation and vibration of the CH_3O fragment.

For a given amount of energy partitioned to translation, conservation of angular momentum requires that a certain amount of energy be partitioned to rotation, which we can calculate within an impulsive model. The angular momentum of the parent radical is negligible, so that the orbital angular momentum, $\vec{L} = \mu\vec{v}_{rel} \times \vec{b}$, arising from the impact parameter, *b*, between the recoiling methoxy radical and chlorine atom, is $\vec{L} \approx -\vec{J}$, where $\vec{J}$ is the angular momentum imparted to methoxy rotation. To estimate the impact parameter *b*, we assume an impulsive kinetic energy release between Cl and the O atom in the methoxy radical portion of the molecule at the ground-state equilibrium geometry of CH_3OCl. For a recoil kinetic energy of 48 kcal/mol, the peak of our measured $P(E_T)$, the model predicts that the rotational angular momentum imparted to the CH_3O moiety is 5.55×10^{-9} J s using the equilibrium geometry of CH_3OCl predicted by Francisco[15] at the CCSD(T)/6-311G-(2df,2p) level of theory, and 5.30×10^{-9} J s using the experimentally determined structure.[35] The values of the impact parameter calculated for these two geometries are 0.682 and 0.652 Å, respectively. The corresponding rotational energy imparted to the CH_3O moiety is 19 and 18 kcal/mol, respectively, calculated from $E_{rot} = \vec{L}^2/2I$, where *I* is the moment of inertia of the CH_3O portion of the molecule about an axis perpendicular to the plane containing the O−Cl bond and the center-of-mass of the CH_3O moiety. (Of course, during the minor geometry change of the CH_3O moiety as it evolves into the CH_3O radical, angular momentum is conserved while *I* changes, so E_{rot} changes slightly.) Thus, around 20 kcal/mol is predicted to be partitioned to rotational energy of the CH_3O fragment when the recoil kinetic energy of the Cl and CH_3O fragments is 48 kcal/mol. This is close to the total internal energy of 21 kcal/mol in the CH_3O fragment. Thus, CH_3O Cl photodissociation at 248 nm produces CH_3O radicals with a very narrow range of internal energies, most of which is in rotational energy. The zero point COCl bending necessarily gives a range of impact parameters, which would spread the range of predicted rotational energies about this estimated value.

Direct dissociation of the O−Cl bond was predicted to be the primary photolysis channel of CH_3OCl in the computational study of Li and Francisco.[14] They calculated potential energy curves for the lowest three singlet and four triplet excited states of CH_3OCl using CASSCF calculations with a pVTZ basis set. All seven excited states were found to be highly repulsive in the O−Cl bond coordinate when this was stretched as other geometrical parameters were held constant. All excited states were either bound or contained an energetic barrier with respect to lengthening of the C−O bond. This suggests that O−Cl bond fission would result from photoexcitation of CH_3OCl, as observed in this experiment. It also suggests that most of the available energy should be partitioned to recoil kinetic energy (except that required to be partitioned to rotation), justifying the impulsive estimate made in the previous paragraph. Indeed, our measured recoil kinetic energy distribution suggests that little energy is partitioned into the CH_3O fragment vibrational energy. This is consistent with the fact that the CH_3O moiety in CH_3OCl has nearly the same equilibrium geometry as the CH_3O radicals; the angles are the same to within 2° and all the bond lengths agree to within 0.02 Å except the C−O bond, which is slightly shorter in the radical.

Qualitatively, our findings are also in accordance with other experimental evidence. The 248 and 308 nm photodissociation of an analogous system to CH_3OCl, *tert*-butyl hypochlorite, was studied with photofragment translational spectroscopy by Thelen et al.[20] The photofragments in that experiment exhibited a fairly narrow translational energy distribution, peaked at 37 kcal/mol, and a value of $\beta = 1.9 \pm 0.1$ following 248 nm photoexcitation, indicating a direct dissociation mechanism. The ultraviolet absorption spectra of a range of hypochlorites show considerable similarities,[13,20] so it is reasonable that alkyl hypochlorites with different alkyl groups would show similar behavior following photoexcitation. However, the energy partitioning to the *tert*-butoxy radical differs qualitatively. The *tert*-butyl hypochlorite recoil kinetic energy distribution is about a factor of 2 broader than that measured here for CH_3OCl (with a fwhm of 8 kcal/mol).[20] The Thelen et al. study of *tert*-butyl hypochlorite also observed decomposition of alkoxy radicals, which occurs with a low energy barrier of ∼20 ± 3 kcal/mol, indicating that a significant amount of the internal energy must have been partitioned to vibration. This is not a surprising result because in the impulsive dissociation the larger *tert*-butoxy radical, with more low-frequency vibrational modes than the CH_3O, is likely to correspond more closely to the soft radical limit, whereas the CH_3OCl photodissociation is closer to the hard radical limit.[36]

Schindler et al.[19] measured a $\Phi = 0.95 \pm 0.05$ quantum yield of Cl + CH_3O after photolysis at 308 nm. Although they did not report a quantum yield following photolysis at 248 nm, they showed that the contributions from HCl elimination and C−O bond fission were negligible, in agreement with this work. The Schindler et al. study also determined the kinetic energy imparted to the chlorine to be 1.29 ± 0.1 eV to $Cl(^2P_{3/2})$ and 1.18 ± 0.1 eV to $Cl(^2P_{1/2})$ after photoexcitation with 235 and 238 nm light, respectively. With conservation of momentum, this implies that the recoil kinetic energy in the center of mass for these systems should be 63.3 ± 3.5 and 57.9 ± 3.5 kcal/mol for $Cl(^2P_{3/2})$ and $Cl(^2P_{1/2})$, respectively. These values were determined from the time lag, Δt, resulting from kinetic energy release in different directions for ionized photofragments under an applied electric field. Because the distribution of photofragments was found to be similar to those of Cl atoms in equilibrium with the carrier gas, the study did not address the width of the recoil kinetic energy distribution of the chlorine atoms. Thus it is most appropriate to compare these recoil kinetic energy values with the peak translational energy value of 48

kcal/mol determined in our experiment. Although the photoexcitation energies are slightly different than the one used in our experiment, they are still all likely to correspond to the $\tilde{X}\ ^1A' \rightarrow 2^1A'$ absorption band. The 235.3 nm dissociating photons for the $Cl(^2P_{3/2})$ channel in the Schindler et al. study resulted in an E_{avl} of only 6.4 kcal/mol larger than our work but found 15.3 kcal/mol more energy partitioned to translation than the current experiment. Such a high translational energy release would not be possible for the equilibrium geometry of CH_3OCl (due to a centrifugal barrier). We presume this discrepancy may be due to the difficulties associated with calibrating kinetic energy release in such turnaround time measurements in the extraction region of a time-of-flight mass spectrometer, although it also could be attributed to differences between the regions of the potential surface accessed by the photons of different wavelengths. The Schindler et al. result for the $Cl(^2P_{1/2})$ channel, excited with a 237.8 nm photon (E_{avl} is 5.2 kcal/mol greater than in our study), is closer to ours; the results almost agree within the combined errors of the two studies.

It is worth considering whether other photodissociation reactions yielding methoxy exhibit comparable energy partitioning to that observed in this study. Two such systems, which have been the subject of several studies, are methyl nitrite (CH_3ONO)[37−40] and methyl hydroperoxide (CH_3OOH).[41−43] Following photodissociation at around 248 nm, these compounds predominantly break into CH_3O, with either an NO or OH cofragment. The energy available after bond cleavage at 248 nm is similar for all systems; about 69 kcal/mol for CH_3OCl, 73.5 kcal/mol for CH_3ONO,[38] and 71 kcal/mol for CH_3OOH.[43] Although the fwhm of the $P(E_t)$ for CH_3OCl is 4 ± 2 kcal/mol, it is much wider for the other two systems, at ∼15 kcal/mol for CH_3ONO,[37] and ∼11 kcal/mol for CH_3OOH. In both CH_3ONO and CH_3OOH, the fact that the internal energy can be partitioned to vibration and rotation of the NO or OH complicates the assignment of the internal energy as compared to the atomic Cl cofragment. The very narrow distribution of recoil kinetic energies of CH_3OCl photofragments, coupled with the fact that virtually all of the energy not partitioned to translation is required by conservation of angular momentum to be partitioned to rotation, implies that the CH_3O fragment has very little vibrational energy, as mentioned before. The forces in the Franck−Condon region of the excited state potential thus must act primarily to stretch the O−Cl bond and the equilibrium geometry of the CH_3O moiety of CH_3OCl is very similar to that of the CH_3O radical. This description is consistent with the characterization of the transition from the ground state to the $2^1A'$ excited state by Li et al., who found it to be primarily from a nonbonding p orbital on Cl to an antibonding orbital composed mainly of s and p orbitals of the O and Cl atoms.[14] In contrast, the S_2 excited state of CH_3ONO has been characterized theoretically by Suter et al., who describe the transition from the ground to S_2 state as predominantly $\pi\pi^*$ and indicate that it is delocalized over the nearly planar π-system of the C−O−N═O portion of the molecule.[39] This could explain why dissociation from the S_2 state of CH_3ONO yields photofragments with a broader distribution of internal energies, as determined from energy conservation and the spread of observed total recoil kinetic energy of the photofragments. Indeed, studies evidence significant partitioning of internal energy to NO vibration.[39,40] The CH_3OOH system also exhibits a much broader recoil kinetic energy release than that measured here for CH_3OCl. Although no calculations have been published for the excited-state potentials of CH_3OOH, Novicki and Vasudev[42] indicate that their observed rotational distribution of the OH fragment is inconsistent with a simple impulsive O−O bond rupture, which would produce a strongly peaked rotational distribution and large positive rotational alignment. Thus, the fact that CH_3OCl photodissociation gives a more narrow energy distribution than either CH_3ONO or CH_3OOH can be explained partially through the difference between atomic and molecular cofragments, and also by considering the forces in the Franck−Condon region.

The current experiment provides direct evidence that methyl hypochlorite undergoes direct dissociation to form $Cl + CH_3O$ upon excitation at 248 nm. The resultant photoproducts are found to be nearly monoenergetic, indicating that methyl hypochlorite could be a useful precursor molecule in studies where $\tilde{X}\ ^2E$ state CH_3O radicals with a narrow range of energies and high rotational excitation are desired. There is much interest in CH_3O apart from its relation to methyl hypochlorite, and a large body of literature, which we will not attempt to review here, has focused on the radical. CH_3O is interesting both theoretically, and because of its importance in combustion and atmospheric systems. CH_3O has been used as a model system for examining the behavior of polyatomics in the study of intramolecular vibrational energy transfer[44] and mode selective photochemistry.[45] The ground state of the radical is subject to Jahn−Teller vibronic coupling as well as spin−orbit coupling and has been used as a prototypical system for the study of these effects.[46,47] The radical is also an important intermediate in high-temperature combustion processes, forming when an oxygen atom reacts with a methyl radical to create CH_3O, which then further decomposes. Several studies have examined the spectroscopy and dynamics of both the $CH_3 + O$ system as well as the photodissociation of CH_3O.[34,46,47] Two product channels have been observed for the $O + CH_3$ reaction, which proceeds through a CH_3O radical intermediate (see review in Marcy et al.[48]). Estimates vary for the branching ratio between these channels, which lead to the products $H + H_2CO$ and $H_2 + HCO$, respectively, where the HCO further dissociates to $H + CO$. Theoretical interaction potentials have been reported by Marcy et al.[48] as well as by Knyazev.[49] The Marcy et al. study predicts a rotational energy dependence of this branching ratio. Generation of the CH_3O radical of this bimolecular reaction with high rotational energy would provide a means of testing these predictions. This study shows that using CH_3OCl as a photolytic precursor for $\tilde{X}$ state CH_3O radicals does not form the CH_3O radical with enough internal vibration to test the Marcy et al. potential surface. However, CH_3OCl photolysis does form $\tilde{X}$ state CH_3O with a very narrow distribution of internal energies, primarily in CH_3O rotation. Experiments that further excite vibrational overtones of the nascent CH_3O radicals could prove useful in probing the intermediate important in large impact parameter $CH_3 + O$ reactive collisions, which produce rotationally excited products. The photodissociation of rotationally exited CH_3O radicals produced from CH_3OCl may also offer an interesting comparison to prior photodissociation studies, such as that by Osborn et al.[47] of the rotationally cold radical.

Acknowledgment. This work was supported by the National Science Foundation, under Grant No. CHE-0109588 (L.J.B.). M.J.K. acknowledges a National Science Foundation Graduate Research Fellowship and L.R.M. was supported in part by a GAANN fellowship. The Advanced Light Source is supported by the Director, Office of Science, Office of Basic Energy Sciences, Materials Sciences Division, of the U.S. Department of Energy under Contract No. DE-AC03-76SF00098 at Lawrence Berkeley National Laboratory. The Chemical Dynamics Beamline is supported by the Director, Office of Science, Office of

Basic Energy Sciences, Chemical Sciences Division of the U.S. Department of Energy under the same contract.

References and Notes

(1) Farman, J. C.; Gardiner, B. G.; Shanklin, J. D. *Nature* **1985**, *315*, 207.
(2) Solomon, S. *Nature* **1990**, *347*, 347.
(3) Anderson, J. G. *Science* **1991**, *251*, 39.
(4) Crutzen, P. J.; Müller, R.; Brühl, C.; Peter, T. *Geophys. Res. Lett.* **1992**, *19*, 1113.
(5) Kenner, R. D.; Ryan, K. R.; Plumb, I. C. *Geophys. Res. Lett.* **1993**, *20*, 1571.
(6) Helleis, F.; Crowley, J. R.; Moortgat, G. K. *J. Phys. Chem.* **1993**, *97*, 11464.
(7) Helleis, F.; Crowley, J.; Moortgat, G. *Geophys. Res. Lett.* **1994**, *21*, 1795.
(8) Simon, F. G.; Burrows, J. P.; Schneider, W.; Moortgat, G. K.; Crutzen, P. J. *J. Phys. Chem.* **1989**, *93*, 7807.
(9) DeMore, W. B. *J. Geophys. Res.* **1991**, *96*, 4995.
(10) Carl, S. A.; Roehl, C. M.; Müller, R.; Moortgat, G. K.; Crowley, J. N. *J. Phys. Chem.* **1996**, *100*, 17191.
(11) Crowley, J. N.; Compuzano-Jost, P.; Moortgat, G. K. *J. Phys. Chem.* **1996**, *100*, 3601.
(12) Crowley, J. N.; Helleis, F.; Müller, R.; Moortgat, G. K.; Crutzen, P. J. *J. Geophys. Res.* **1994**, *99*, 20683.
(13) Jungkamp, T. P. W.; Kirchner, U.; Schmidt, M.; Schindler, R. N. *J. Photochem. Photobiol., A* **1995**, *91*, 1.
(14) Li, Y.; Francisco, J. S. *J. Chem. Phys.* **1999**, *111*, 8384.
(15) Francisco, J. S. *Int. J. Quantum Chem.* **1999**, *73*, 29.
(16) Espinosa-Gárcia, J. *Chem. Phys. Lett.* **1999**, *315*, 239.
(17) He, T.-J.; Chen, D.-M.; Liu, F.-C.; Sheng, L.-S. *Chem. Phys. Lett.* **2000**, *332*, 545.
(18) Jung, D.; Chen, C.-J.; Bozzelli, J. W. *J. Phys. Chem. A* **2000**, *104*, 9581.
(19) Schindler, R. N.; Liesner, M.; Schmidt, S.; Kirchner, U.; Benter, T. *J. Photochem. Photobiol., A* **1997**, *107*, 9.
(20) Thelen, M.-A.; Felder, P.; Frey, J. G.; Huber, J. R. *J. Phys. Chem.* **1993**, *97*, 6220.
(21) Jenner, E. L. *J. Org. Chem.* **1962**, *27*, 1031.
(22) Mintz, M. J.; Walling, C. *Organic Syntheses*; Wiley: New York, 1973; Vol. 5, pp 184−187.
(23) Heimann, P. A.; Koike, M.; Hsu, C. W.; Blank, D.; Yang, X. M.; Suits, A. G.; Lee, Y. T.; Evans, M.; Ng, C. Y.; Flaim, C.; Padmore, H. A. *Rev. Sci. Instrum.* **1997**, *68*, 1945.
(24) Yang, X.; Lin, J.; Lee, Y. T.; Blank, D. A.; Suits, A. G.; Wodtke, A. M. *Rev. Sci. Instrum.* **1997**, *68*, 3317.
(25) Peterka, D.; Ahmed, M. Personal communication, 2002.
(26) Hubrich, C.; Stuhl, F. *J. Photochem.* **1980**, *12*, 93.
(27) Frisch, M. J.; Trucks, G. W.; Schlegel, H. B.; Scuseria, G. E.; Robb, M. A.; Cheeseman, J. R.; Zakrzewski, V. G.; Montgomery, J. A., Jr.; Stratmann, R. E.; Burant, J. C.; Dapprich, S.; Millam, J. M.; Daniels, A. D.; Kudin, K. N.; Strain, M. C.; Farkas, O.; Tomasi, J.; Barone, V.; Cossi, M.; Cammi, R.; Mennucci, B.; Pomelli, C.; Adamo, C.; Clifford, S.; Ochterski, J.; Petersson, G. A.; Ayala, P. Y.; Cui, Q.; Morokuma, K.; Rega, N.; Salvador, P.; Dannenberg, J. J.; Malick, D. K.; Rabuck, A. D.; Raghavachari, K.; Foresman, J. B.; Cioslowski, J.; Ortiz, J. V.; Baboul, A. G.; Stefanov, B. B.; Liu, G.; Liashenko, A.; Piskorz, P.; Komaromi, I.; Gomperts, R.; Martin, R. L.; Fox, D. J.; Keith, T.; Al-Laham, M. A.; Peng, C. Y.; Nanayakkara, A.; Challacombe, M.; Gill, P. M. W.; Johnson, B.; Chen, W.; Wong, M. W.; Andres, J. L.; Gonzalez, C.; Head-Gordon, M.; Replogle, E. S.; Pople, J. A. *Gaussian 98*, revision A.11.3; Gaussian, Inc.: Pittsburgh, PA, 2002.
(28) Baboul, A. G.; Curtiss, L. A.; Redfern, P. C.; Raghavachari, K. *J. Chem. Phys.* **1999**, *110*, 7650.
(29) Kuo, S.-C.; Zhang, Z.; Klemm, R. B.; Liebman, J. F.; Stief, L. J.; Nesbitt, F. L. *J. Phys. Chem.* **1994**, *98*, 4026.
(30) Ruscic, B.; Berkowitz, J. *J. Chem. Phys.* **1991**, *95*, 4033.
(31) Harvey, J. N.; Aschi, M. *Phys. Chem. Chem. Phys.* **1999**, *1*, 5555.
(32) Traeger, J. C. *Int. J. Mass Spectrom. Ion Processes* **1985**, *66*, 271.
(33) Liu, X.; Damo, C. P.; Lin, T.-Y. D.; Foster, S. C.; Misra, P.; Yu, L.; Miller, T. A. *J. Phys. Chem.* **1989**, *93*, 2266.
(34) Powers, D. E.; Pushkarsky, M. B.; Miller, T. A. *J. Chem. Phys.* **1997**, *106*, 6863.
(35) Rigden, J. S.; Butcher, S. S. *J. Chem. Phys.* **1964**, *40*, 2109.
(36) Riley, S. J.; Wilson, K. R. *Faraday Discuss.* **1972**, *53*, 132.
(37) Keller, B. A.; Felder, P.; Huber, J. R. *Chem. Phys. Lett.* **1986**, *124*, 135.
(38) Keller, B. A.; Felder, P.; Huber, J. R. *J. Phys. Chem.* **1987**, *91*, 1114.
(39) Suter, H. U.; Brühlmann, U.; Huber, J. R. *Chem. Phys. Lett.* **1990**, *171*, 63.
(40) Yin, H.-M.; Sun, J.-L.; Li, Y.-M.; Han, K.-L.; He, G.-Z. *J. Chem. Phys* **2003**, *118*, 8248.
(41) Vaghhiani, G. L.; Ravishankara, A. R. *J. Chem. Phys.* **1990**, *92*, 996.
(42) Novicki, S. W.; Vasudev, R. *J. Chem. Phys.* **1990**, *93*, 8725.
(43) Thelen, M.-A.; Felder, P.; Huber, J. R. *Chem. Phys. Lett.* **1993**, *213*, 275.
(44) Geers, A.; Kappert, J.; Temps, F.; Wiebrecht, J. W. *J. Chem. Phys.* **1994**, *101*, 3634.
(45) Powers, D. E.; Pushkarsky, M. B.; Miller, T. A. *J. Chem. Phys.* **1997**, *106*, 6878.
(46) Temps, F. Vibrational spectroscopy, intramolecular dynamics and state specific unimolecular dissociation of CH_3O (X^2E). In *Molecular Dynamics and Spectroscopy by Stimulated Emission Pumping*; Dai, H. L., Field, R. W., Eds.; World Scientific: Singapore, 1995; Vol. 4, p 375.
(47) Osborn, D. L.; Leahy, D. J.; Neumark, D. M. *J. Phys. Chem. A* **1997**, *101*, 6583.
(48) Marcy, T. P.; Díaz, R. R.; Heard, D.; Leone, S. R.; Harding, L. B.; J., K. S. *J. Phys. Chem. A* **2001**, *105*, 8361.
(49) Knyazev, V. D. *J. Phys. Chem. A* **2002**, *106*, 8741.